

## A facile synthesis of UiO-66, UiO-67 and their derivatives†

Cite this: *Chem. Commun.*, 2013, **49**, 9449

Received 9th August 2013,  
Accepted 28th August 2013

DOI: 10.1039/c3cc46105j

www.rsc.org/chemcomm

**A scalable, reproducible method of synthesizing UiO-66- and UiO-67-type MOFs, entailing the addition of HCl to the reaction mixture, has been investigated. The new protocol requires a fraction of the time of previously reported procedures, yields exceptional porosities, and works with a range of linkers.**

Metal–organic frameworks (MOFs)<sup>1</sup> are a class of porous materials composed of organic struts joined with inorganic nodes. MOFs have been studied extensively, and due to the wide variety of organic linkers, they may be tailored to many applications such as gas storage<sup>2</sup> and separation,<sup>3</sup> catalysis,<sup>4</sup> chemical sensing,<sup>5</sup> ion exchange,<sup>6</sup> drug delivery,<sup>7</sup> and light harvesting.<sup>8</sup> One of the most attractive aspects of MOF synthesis is that the organic bridging ligand can be synthetically modified in order to introduce a desired functionality to the framework. However, there are limitations to this approach and new conditions may need to be worked out for modifications.

In the scope of our on-going investigations into the application of MOFs for separations and catalysis, we turned our attention to Zr-cluster-based MOFs due to their excellent thermal, aqueous, and acid stability (Fig. 1).<sup>9–16</sup> Several derivatives of these MOFs have been synthesized with linkers possessing functional groups such as amines, halogens, hydroxyls, or nitros.<sup>2,16,17</sup> UiO-66 and UiO-67 are two Zr-based frameworks used most often.<sup>18</sup> UiO-66 consists of a cubic framework of cationic  $\text{Zr}_6\text{O}_4(\text{OH})_4$  nodes (formed *in situ* via hydrolysis of  $\text{ZrCl}_4$ ) and 1,4-benzenedicarboxylate linkers (BDC).<sup>14,18,19</sup> UiO-67 has a similar structure, except it utilizes biphenyl-4,4'-dicarboxylate (BPDC) linkers instead of BDC (Fig. 1).<sup>18</sup> The structure contains two types of cages: an octahedral cage (Fig. 1, large purple sphere) that is face sharing with 8 tetrahedral cages (Fig. 1, small purple spheres) and edge sharing with 8 additional octahedral pores.

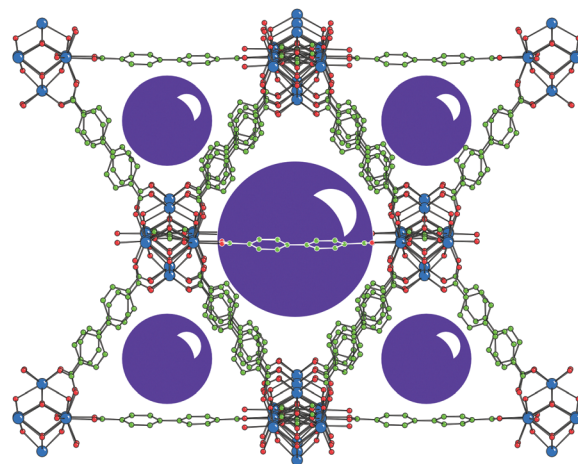


**Fig. 1** The structure of UiO-67 showing a single octahedral cage (large sphere). The face of each octahedral is shared with 8 smaller tetrahedral cages (small spheres).

Oftentimes, in our hands, synthesizing UiO-66 derivatives having a desired functionality has not been straightforward. To that end, post-synthesis decoration of UiO-66-NH<sub>2</sub>, and Solvent-Assisted Linker Exchange (SALE) have been previously demonstrated as powerful tools to modify UiO-66 or UiO-66-NH<sub>2</sub>.<sup>17,20–22</sup> Unfortunately, our attempts to synthesize UiO-66-NH<sub>2</sub> via several direct protocols were inconsistent, occasionally yielding a non-porous amorphous material. No obvious factor could be identified to account for batch-to-batch differences.<sup>23</sup> We were interested in developing a linker-general protocol by which UiO-66(67) derivatives could consistently be formed *de novo*.<sup>24</sup> We thus examined the utility of concentrated HCl in the formation of UiO-type MOFs (see Table 1, Fig. 3 and 4, and ESI†); we speculate that the role of the HCl is either to condition the solvent (*N,N*-dimethylformamide, DMF) by neutralizing basic impurities (amines) and/or to assist in forming hexa-Zr clusters prior to linker binding. Reproducible results were obtained when a half-filled 8-dram vial containing a 1:1.4 molar ratio of  $\text{ZrCl}_4$  (0.54 mmol pre-dissolved in 5:1 v:v DMF:HCl) to benzene-dicarboxylic acid ( $\text{H}_2\text{BDC}$ ; pre-dissolved in 10 mL DMF) was heated at 80 °C overnight.<sup>25</sup> A fine white powder settles after several hours (see Fig. 2). Notably, a 50-fold scale up exhibited no change in product crystallinity or porosity (see Fig. S13, ESI†).

<sup>a</sup> Department of Chemistry, Northwestern University, 2145 Sheridan Road, Evanston, Illinois 60208, USA. E-mail: o-farha@northwestern.edu, j-hupp@northwestern.edu; Tel: +1-847-491-3504

<sup>b</sup> Department of Chemical & Biological Engineering, Northwestern University, 2145 Sheridan Road, Evanston, Illinois 60208, USA

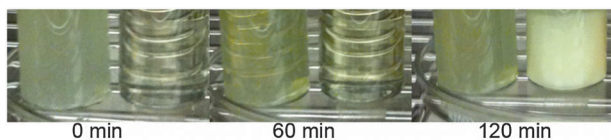
† Electronic supplementary information (ESI) available: Experimental details, PXRD of UiO-67, TGA analysis, simulated isotherms, and IR spectra of UiO-66. See DOI: 10.1039/c3cc46105j

‡ These authors contributed equally.

**Table 1** Observed and calculated BET surface areas

Compound	Experimental N <sub>2</sub> BET SA (m <sup>2</sup> g <sup>-1</sup> )	Calculated geometric SA with 12 linkers per node (m <sup>2</sup> g <sup>-1</sup> )	Calculated geometric SA with 8 linkers per node (m <sup>2</sup> g <sup>-1</sup> )
UiO-66	1580	800 <sup>c</sup>	1550 <sup>d</sup>
UiO-66-NH <sub>2</sub>	830 <sup>a</sup> /1200	700	1150
UiO-66-(NH <sub>2</sub> ) <sub>2</sub>	540	450	— <sup>b</sup>
UiO-66-OH	1000	600	1250
UiO-66-(OH) <sub>2</sub>	560	400	— <sup>b</sup>
UiO-66-NO <sub>2</sub>	860	500	1100
UiO-67	2500	2700	3100
UiO-67-NO <sub>2</sub>	2160	2000	— <sup>b</sup>
UiO-67-NH <sub>2</sub>	2080	2150	— <sup>b</sup>

<sup>a</sup> HCl free synthesis. <sup>b</sup> Due to agreement between observed and 12-linker calculated surface areas, geometric SAs for missing-linker versions were not calculated. <sup>c</sup> A BET SA of 1100 m<sup>2</sup> g<sup>-1</sup> was obtained by fitting simulated isotherms. <sup>d</sup> A BET SA of 1400 m<sup>2</sup> g<sup>-1</sup> was obtained by fitting simulated isotherms.

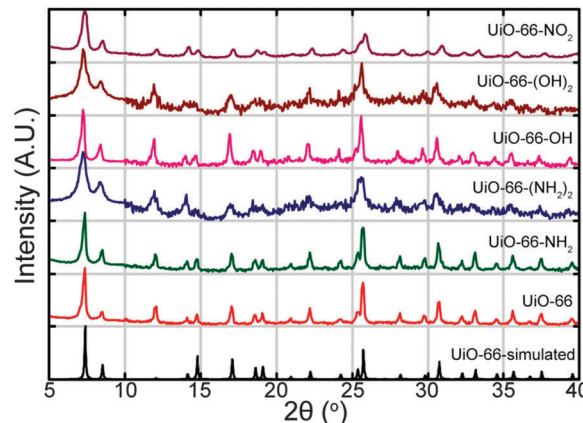
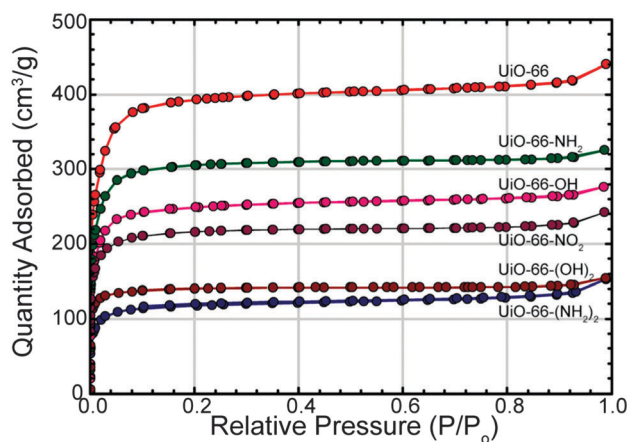
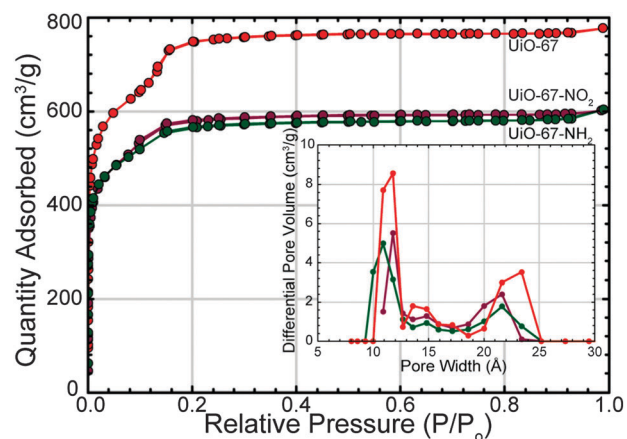
**Fig. 2** HCl-free synthesis (left) and HCl-containing synthesis (right).

To gain mechanistic insight, the formation of UiO-66 was visually monitored with and w/o HCl. We initially observed the solubility of ZrCl<sub>4</sub> in DMF is enhanced by HCl. Secondly, HCl speeds product formation; after 2 h, a precipitate of UiO-66 is formed in an HCl-containing vial, whereas none is observed in an HCl-free vial (Fig. 2). Apart from shorter or longer reaction time, syntheses at 120 or 60 °C were similarly successful. The rest of the work presented herein is for syntheses at 80 °C.<sup>26</sup> Decreasing the amount of HCl (Fig. S3, ESI†) slowed down MOF formation and decreased the surface area (SA, Fig. S4, ESI†). We postulate that the presence of nearly 1.5 equivalence of BDC per Zr may prevent nodes from joining each other. HCl aids in dissociating linkers from nodes and ultimately speeds up the connection of nodes to one another. While typically acid slows down MOF formation, it speeds up formation for the case of UiO-66.<sup>14</sup>

In order to determine the synthetic generality of this protocol, we extended the investigation to five UiO-66 derivatives: UiO-66-NH<sub>2</sub>, UiO-66-(NH<sub>2</sub>)<sub>2</sub>, UiO-66-OH, UiO-66-(OH)<sub>2</sub>,<sup>22</sup> and UiO-66-NO<sub>2</sub>. Table 1 and Fig. 3 and 4 summarize or show PXRD and isotherm data for the parent and putative derivative compounds. The PXRD results clearly show that all five derivative compounds are isostructural with UiO-66. In our lab only UiO-66 and UiO-66-NH<sub>2</sub> (intermittently) proved accessible *via* standard literature procedures. Brunauer–Emmett–Teller (BET) SAs of 1200, 540, 1000, 560, and 860 m<sup>2</sup> g<sup>-1</sup> were observed, respectively, for UiO-66-NH<sub>2</sub>, UiO-66-(NH<sub>2</sub>)<sub>2</sub>, UiO-66-OH, UiO-66-(OH)<sub>2</sub>, and UiO-66-NO<sub>2</sub> (Fig. 4, Table 1).

Under this approach, we were also able to synthesize UiO-67 (BPDC linkers), UiO-67-NO<sub>2</sub>, and UiO-67-NH<sub>2</sub> (see Fig. S2, ESI† for PXRDs).<sup>27</sup> BET SAs were 2500, 2160, and 2080 m<sup>2</sup> g<sup>-1</sup> (Fig. 5, Table 1). Interestingly, the SAs of the activated materials did not change when they were left for a week on the bench, implying no degradation for at least a week.<sup>28</sup>

The isotherms of all three UiO-67 derivatives show a step at *ca.* 0.1 *P/P*<sub>0</sub> due to the presence of two types of pores (Fig. 1). Pore size distribution analyses indicated that the octahedral pore has a

**Fig. 3** Simulated (black) and observed PXRD patterns of UiO-66 and derivatives; the intensity from 10–40° is enhanced 10× for clarity.**Fig. 4** Nitrogen isotherms of UiO-66 and derivatives at 77 K.**Fig. 5** N<sub>2</sub> isotherms of UiO-67 and derivatives at 77 K. Inset shows pore-size distribution as determined *via* DFT (carbon slit pore N<sub>2</sub> 77 K kernel).

diameter of 23, 21, or 21.5 Å, while the diameter of the tetrahedral pore is 11.5, 12, or 11 Å, respectively for UiO-67, UiO-67-NO<sub>2</sub>, UiO-67-NH<sub>2</sub> (Fig. 5).<sup>29</sup> These values are consistent with X-ray structural data. Comparing the BET SAs obtained with the HCl protocol (Table 1) with literature values shows that the HCl protocol yields unusually high values.<sup>10,14,30</sup> Extant UiO-66 preparations have yielded SAs of *ca.* 700–1400 m<sup>2</sup> g<sup>-1</sup>,<sup>14</sup> versus 1600 m<sup>2</sup> g<sup>-1</sup> here. For UiO-66-NH<sub>2</sub>,

the average of several reported SAs is  $850 \text{ m}^2 \text{ g}^{-1}$ , with one reaching  $1206 \text{ m}^2 \text{ g}^{-1}$ .<sup>9,30,31</sup> We obtained  $1200 \text{ m}^2 \text{ g}^{-1}$ . Remarkably, for several of the MOFs examined here, SAs derived from computationally simulated  $\text{N}_2$  isotherms or from geometric modeling of ideal crystals are smaller than observed experimentally (Table 1).

Our working explanation for the unexpectedly large experimental SAs is that a small fraction of linkers are absent (Fig. S5, S8 and S9, ESI†).<sup>19,32,34,35</sup> Theoretical work by Sarkisov and Harrison has shown that when small linkers (such as BDC) are missing, calculated SAs increase.<sup>33</sup> We find for several UiO MOFs that calculated SAs show good agreement with experimental (Table 1) if four of twelve node linkers are assumed missing. In order to probe the presence of missing linkers, we examined the elemental analysis (EA), pore size distribution analysis, PXRD, and thermogravimetric analysis (TGA) of UiO-66.<sup>14</sup> Elemental analysis (Table S2, ESI†) illustrates that in the HCl-containing synthesis there is more zirconium and less carbon content than in UiO-66 made *via* the conventional route.<sup>14</sup> Consistent with missing linkers, pore size distribution demonstrates that the smaller tetrahedral pore shifts from *ca.*  $8.5 \text{ \AA}$  to *ca.*  $11.5 \text{ \AA}$  (Fig. S5, ESI†). Furthermore, calculated and observed PXRDs indicate that the 200 reflection is systematically more intense when linkers are missing (Fig. S6, ESI†). TGA of UiO-66 and UiO-67 (Fig. S8 and S9, ESI†) are characterized by a mass loss between 500 and  $600^\circ\text{C}$  that is attributable to linker volatilization. Notably, the amount lost is *ca.* 10% less than expected if the compounds have full complements of linkers.

Finally, eliminating anionic BDC units from UiO-66 necessitates that clusters add oxo, hydroxo, aquo, or chloro ligands. Consistent with this idea, the IR spectrum (Fig. S12, ESI†) of UiO-66 made *via* the HCl route displays more peaks in the O–H stretching region than does the conventionally prepared material; EA indicated that only 10% of the vacant sites contain a chloride anion. The combination of experimental and theoretical data is consistent with the hypothesis that the procedure described herein produces linker defect sites in UiO-66 and some analogues.

Including HCl in reaction mixtures during the syntheses of UiO-66(67)-type MOFs reliably yielded products corresponding to each of the nine materials targeted. Notably, some of these materials had proven inaccessible by existing direct-synthesis protocols. With HCl, we find that the syntheses can be greatly accelerated and that they can scaled-up 50-fold without loss of crystallinity or porosity.  $\text{N}_2$  SAs for several of the studied compounds exceed the highest values expected theoretically based on ideal crystals. The experimental SAs can be computationally replicated, however, by assuming that each hexa-Zr node coordinates  $\sim 8$  linkers, rather than 12. TGA data provide support for this explanation, while IR data imply that linker-vacated sites are occupied by hydroxide ions.

OKF, JTH and RQS gratefully acknowledge DTRA for financial support (grant HDTRA1-10-1-0023). YJC gratefully acknowledges the NSF Graduate Research Fellowship (grant DGE-0824162).

## Notes and references

- (a) M. O'Keeffe, M. A. Peskov, S. J. Ramsden and O. M. Yaghi, *Acc. Chem. Res.*, 2008, **41**, 1782; (b) G. Férey, *Chem. Soc. Rev.*, 2008, **37**, 191; (c) S. Horike, S. Shimomura and S. Kitagawa, *Nat. Chem.*, 2009, **1**, 695.
- (a) L. J. Murray, M. Dincă and J. R. Long, *Chem. Soc. Rev.*, 2009, **38**, 1294; (b) J. Sculley, D. Yuan and H.-C. Zhou, *Energy Environ. Sci.*, 2011, **4**, 2721.
- (a) J.-R. Li, R. J. Kuppler and H.-C. Zhou, *Chem. Soc. Rev.*, 2009, **38**, 1477; (b) J. An, S. J. Geib and N. L. Rosi, *J. Am. Chem. Soc.*, 2010, **132**, 38; (c) Y.-S. Bae, A. M. Spokoyny, O. K. Farha, R. Q. Snurr, J. T. Hupp and C. A. Mirkin, *Chem. Commun.*, 2010, **46**, 3478; (d) D. Britt, H. Furukawa, B. Wang, T. G. Glover and O. M. Yaghi, *Proc. Natl. Acad. Sci. U. S. A.*, 2009, **106**, 20637.
- (a) L. E. Kreno, A. M. Shultz, A. A. Sarjeant, S. T. Nguyen and J. T. Hupp, *J. Am. Chem. Soc.*, 2011, **133**, 5652; (b) L. Ma, C. Abney and W. Lin, *Chem. Soc. Rev.*, 2009, **38**, 1248; (c) J. Lee, O. K. Farha, J. Roberts, K. A. Scheidt, S. T. Nguyen and J. T. Hupp, *Chem. Soc. Rev.*, 2009, **38**, 1450.
- (a) L. E. Kreno, K. Leong, O. K. Farha, M. Allendorf, R. P. Van Duyne and J. T. Hupp, *Chem. Rev.*, 2012, **112**, 1105; (b) M. D. Allendorf, C. A. Bauer, R. K. Bhakta and R. J. T. Houk, *Chem. Soc. Rev.*, 2009, **38**, 1330.
- J. An and N. L. Rosi, *J. Am. Chem. Soc.*, 2010, **132**, 5578.
- (a) J. Della Rocca, D. Liu and W. Lin, *Acc. Chem. Res.*, 2011, **44**, 957; (b) P. Horcajada, C. Serre, M. Vallet-Regí, M. Sebban, F. Taulelle and G. Férey, *Angew. Chem., Int. Ed.*, 2006, **45**, 5974.
- (a) C. Y. Lee, O. K. Farha, B. J. Hong, A. A. Sarjeant, S. T. Nguyen and J. T. Hupp, *J. Am. Chem. Soc.*, 2011, **133**, 15858; (b) C. A. Kent, B. P. Mehl, L. Ma, J. M. Papanikolas, T. J. Meyer and W. Lin, *J. Am. Chem. Soc.*, 2010, **132**, 12767.
- P. M. Schoencker, G. A. Belancik, B. E. Grabicka and K. S. Walton, *AIChE J.*, 2012, **59**, 1255.
- S. Biswas and P. Van Der Voort, *Eur. J. Inorg. Chem.*, 2013, 2154.
- J. B. DeCoste, G. W. Peterson, H. Jasuja, T. G. Glover, Y.-G. Huang and K. S. Walton, *J. Mater. Chem. A*, 2013, **1**, 5642.
- M. Kandiah, M. H. Nilsen, S. Usseglio, S. Jakobsen, U. Olsbye, M. Tilset, C. Larabi, E. A. Quadrelli, F. Bonino and K. P. Lillerud, *Chem. Mater.*, 2010, **22**, 6632.
- H. Wu, T. Yildirim and W. Zhou, *J. Phys. Chem. Lett.*, 2013, **4**, 925.
- A. Schaate, P. Roy, A. Godt, J. Lippke, F. Waltz, M. Wiebecke and P. Behrens, *Chem.-Eur. J.*, 2011, **17**, 6643.
- V. Guillermin, F. Ragon, M. Dan-Hardi, T. Devic, M. Vishnuvarthan, B. Campo, A. Vimont, G. Clet, Q. Yang, G. Maurin, G. Férey, A. Vittadini, S. Gross and C. Serre, *Angew. Chem.*, 2012, **51**, 9267.
- Y. Huang, W. Qin, Z. Li and Y. Li, *Dalton Trans.*, 2012, **41**, 9283.
- M. Kim, S. J. Garibay and S. M. Cohen, *Inorg. Chem.*, 2011, **50**, 729.
- J. H. Cavka, S. Jakobsen, U. Olsbye, N. Guillou, C. Lamberti, S. Bordiga and K. P. Lillerud, *J. Am. Chem. Soc.*, 2008, **130**, 13850.
- L. Valenzano, B. Civalieri, S. Chavan, S. Bordiga, M. H. Nilsen, S. Jakobsen, K. P. Lillerud and C. Lamberti, *Chem. Mater.*, 2011, **23**, 1700.
- S. J. Garibay and S. M. Cohen, *Chem. Commun.*, 2010, **46**, 7700.
- M. Kandiah, S. Usseglio, S. Svelle, U. Olsbye, K. P. Lillerud and M. Tilset, *J. Mater. Chem.*, 2010, **20**, 9848.
- M. Kim, J. F. Cahill, Y. Su, K. A. Prather and S. M. Cohen, *Chem. Sci.*, 2012, **3**, 126.
- Attempts under seemingly identical conditions yielded a pale yellow material with the correct PXRD and SA (Fig. S1, ESI†). The amorphous material was found to dissolve when stirred in a solution of DMF and HCl for several hours (200 mg MOF, 15 mL DMF, 1 mL HCl). Subsequent heating to  $80^\circ\text{C}$  for 3 hours produced a pale-yellow powder having a consistent PXRD and SA to UiO-66- $\text{NH}_2$  ( $830 \text{ m}^2 \text{ g}^{-1}$ ).
- Many literature protocols contain different types and amounts of acids, temperatures, and even different reaction vessels.
- Dissolving the ligand first, or mixing all reagents before heating, produced UiO-66 samples with lower surface area.
- A  $200 \text{ m}^2 \text{ g}^{-1}$  variation in SA was observed over the temperature range.
- HCl has been previously shown to be detrimental in the synthesis of UiO-67 (see ref. 14). The higher concentration and molar ratio of HCl in our synthesis is likely responsible for the difference.
- UiO-67- $\text{NH}_2/\text{NO}_2$  when activated *via* supercritical  $\text{CO}_2$  did not degrade over the course of a week. When conventional heating under vacuum was employed ( $100^\circ\text{C}$ ), low initial SA was observed (Fig. S1, ESI†) followed by collapse of the framework after a week; it is unclear why these methods produce such stark differences in stability.
- DFT, carbon slit pore  $\text{N}_2$  77 K kernel.
- O. G. Nik, X. Y. Chen and S. Kaliaguine, *J. Membr. Sci.*, 2012, **413–414**, 48.
- C. Zlotea, D. Phanon, M. Mazaj, D. Heurtaux, V. Guillermin, C. Serre, P. Horcajada, T. Devic, E. Magnier, F. Cuevas, G. Férey, P. L. Llewellyn and M. Latroche, *Dalton Trans.*, 2011, **40**, 4879.
- J. Park, Z. U. Wang, L.-B. Sun, Y.-P. Chen and H.-C. Zhou, *J. Am. Chem. Soc.*, 2012, **134**, 20110.
- L. Sarkisov and A. Harrison, *Mol. Simul.*, 2011, **37**, 1248.
- F. Vermoortele, B. Bueken, G. Le Bars, B. Van de Voorde, M. Vandichel, K. Houthoofd, A. Vimont, M. Daturi, M. Waroquier, V. Van Speybroeck, C. Kirschhock and D. E. De Vos, *J. Am. Chem. Soc.*, 2013, **31**, 11465.
- H. Wu, Y. S. Chua, V. Krungleviciute, M. Tyagi, P. Chen, T. Yildirim and W. Zhou, *J. Am. Chem. Soc.*, 2013, **28**, 10525.